Magazine of Civil Engineering. 2026. 19(1). Article No. 14107

Magazine of Civil Engineering

ISSN 2712-8172

journal homepage: http://engstroy.spbstu.ru/

Research article

UDC 624

DOI: 10.34910/MCE.141.7

Finite element analysis of the effect reinforced concrete beams under pure torsion strengthened by SIFCON jacketing with different fiber types

M.J. Mohammed [1]✉ **, A.A. Al-Azzawi**[2]

[1]*Department of Civil Engineering, College of Engineering, Al-Nahrain University, Baghdad, Iraq*
[2]*Department of Forensic Engineering, Higher Institute of Forensic Sciences, Al-Nahrain University, Jadriya, Baghdad, Iraq*

✉ *st.Mohammed.g.m.f@nahrainuniv.edu.iq*

Keywords: Pure Torsion, Slurry Infiltrated Fiber Concrete, SIFCON, Strengthening Layer, Hybrid Fibers, Finite Element.

Abstract. In recent years, emphasis has been made on studying the effect and behavior of beams under pure torsion, which required the emergence of different types of strengthening. Because of concrete's poor tensile strength, fiber can be added with high or low percentages. This paper aimed to study the torsional behavior of reinforced concrete beams and the jacketing technique. Reinforced beams were strengthened using a layer of Slurry Infiltrated Fiber Concrete (SIFCON) and with different types of fiber. SIFCON is a special type of fiber concrete that contains a high percentage of fiber. It is an effective substance used for repair and strengthening. The finite element (FE) method through ABAQUS software is carried out to test seven samples previously tested experimentally. Reasonable agreement was acquired between the ultimate torque and angle of twist of FE numerical models and found experimentally, in which the value of the mean and coefficient of variations were 0.998 and 0.247 %, respectively for the ultimate torque, whilst for the angle of twist, the value of the mean and coefficient of variation were 0.945 and 3.823 %, respectively. The effect of increasing longitudinal reinforcement ratio is found to be higher for torsional unreinforced beams and marginal for other beams for the selected range of reinforcement ratio or diameter (8 to 12 mm bar diameter). The effect of thickness of the SIFCON layer on the behavior is found to be higher for steel fiber SIFCON and lower for hybrid fiber SIFCON jacketing. The effect of hybrid fiber on behavior is studied.

Citation: Mohammed, M.J., Al-Azzawi, A.A. Finite element analysis of the effect reinforced concrete beams under pure torsion strengthened by SIFCON jacketing with different fiber types. Magazine of Civil Engineering. 2026. 19(1). Article no. 14107. DOI: 10.34910/MCE.141.7

1. Introduction

Reinforced concrete (RC) beams are one of the fundamentals that transfer building loads, so it is necessary to study their properties and behavior. Buildings made of concrete are prone to torsion [1]. When exposed to extreme torsion, concrete beams can lose strength, the concrete cover can break off, crack, and less efficient steel reinforcing or collapses the structure. So, it is necessary to find a way to strengthen beams. Effective strengthening may be performed on concrete beams for them to increase their structural performance. Two methods can be subjected to strengthening RC beams [1] internal by using fiber to cast beams or cast layer within (2) externally by using a precast layer or by casting a strengthening layer on beams. This method's efficiency enhances the torsional capacity, Slurry Infiltrated Fiber Concrete (SIFCON) is included in fiber at a volume-relative level of 4–20 % [2, 3].

Ali [4] studied finite element (FE) analysis for beams under pure torsion; she studied RC beams strengthened with near-surface mounted (NSM) reinforcement bars by using ABAQUS. Results from the numerical analysis were in good agreement with those from the experimental investigation. The failure and final torque patterns and processes showed this convergence. The ultimate torque increased by approximately 18.06 % for beams with torsional reinforcement. At the same time, it increased by about 9.62 % for beams without torsional reinforcement strengthening with four faces of double NSM U stirrups. When strengthening configurations with four faces of NSM closed stirrups and three faces of NSM stirrups (U-shape) at a spacing of 130 mm, respectively. Beams with torsional reinforcement were identified as the most effective system for strengthening RC beams of torsion resistance.

Le and Coa [5] investigated the torsional effect of circular steel tubes filled with concrete (CFST) under pure torsion numerically. CFST numerical models were created in ABAQUS which describe the mechanism of torsional stress transmission from steel plates to CFST. The parametric study's findings showed that while concrete avoided buckling and enhanced the efficiency of the steel tubes, its compressive strength only slightly increased the torsional moment capacity of the CFST. The yield torsional moment of the CFST rose by around 50 % when the yield strength of steel increased from 235 to 420 MPa.

Majed et al. [6] used of composite materials to reinforce structural components has gained a lot of interest. Under pure torsion, the response of rectangular RC reinforced with fiber-reinforced polymer (FRP) laminates was examined numerically and verified. Parametric research was conducted, taking into account variables including the amount of FRP plies, the compressive strength of the concrete, and the orientation of FRP strips. The findings demonstrated that by raising the number of FRP plies and the compressive strength of the concrete, the torsional capacity could be improved. Furthermore, no discernible difference in the torsional strength of RC beams reinforced with a 45 or 90 ° FRP laminate was found.

The failure mode of RC structural members retrofitted by FRP can be changed, while torsion plays a vital role in loading. Ganganagoudar et al. [7] presented an analytical and FE study to propose a modified softened membrane model for torsion (SMMT-FRP). Their results proved an increase in structural behavior such as post-cracking stiffness, ultimate strength, and localized damage of RC retrofitted members, also showed agreement with Jain et al. [8]. This paper will use strengthened by using SIFCON.

To determine the efficiency of the strengthening layer of SIFCON with different fiber types of RC beams under pure torsion, this research used the ABAQUS program, as it is a very important program in an analytical study of this method. The study concentrated on the effects of normal concrete (NC) compressive strength, reinforcement diameter bar, thickness of the SIFCON layer, different percepts of steel fiber (SF) and glass fiber (GB) within the hybrid fiber (HF), length of the strengthening SIFFCON layer.

2. Methods

2.1. Modeling

2.1.1. Parts

A simply supported beam with a span of 2000 mm a section height of 250 mm and a width of 100 mm, cover of a beam of 20 mm shown in Fig. 1 [9]. In ABAQUS, the concrete adopted C3D8R element as shown in Figs. 2 to 5 (NC beams).

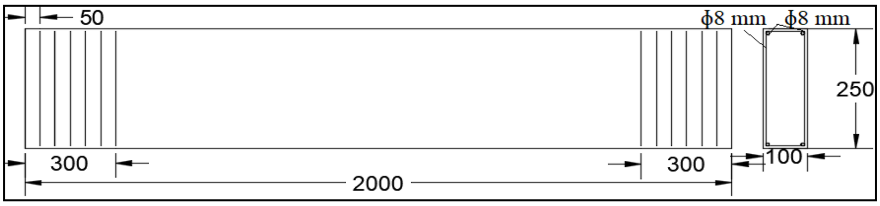

a)

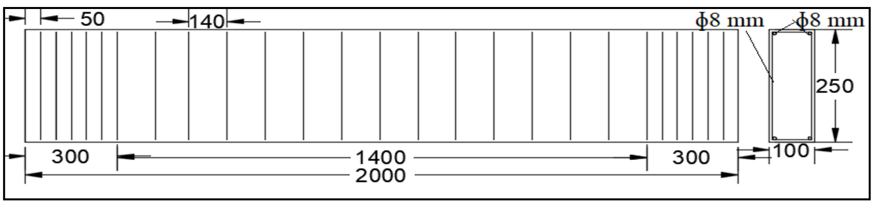

b)

Figure 1. Reinforcement details of beams: a) BN, BSSSFa, BSSSFb, BSSHFa, BSSHFb, BSSGF; and b) BW.

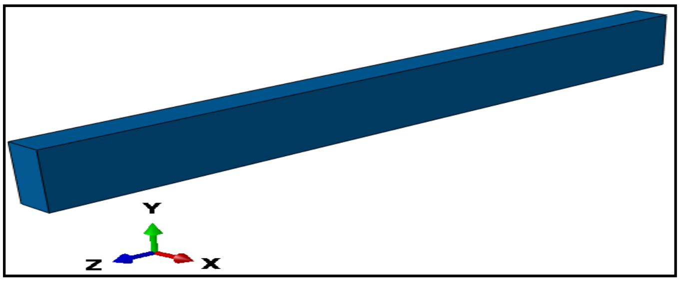

Figure 2. Normal concrete beam.

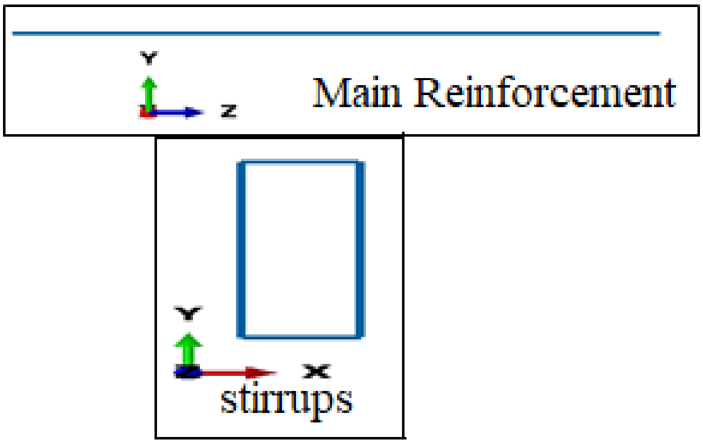

Figure 3. Main and stirrups reinforcement.

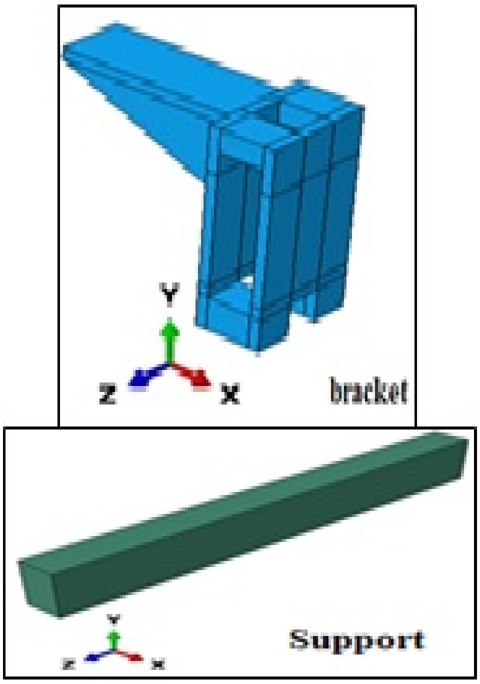

Figure 4. Bracket and support.

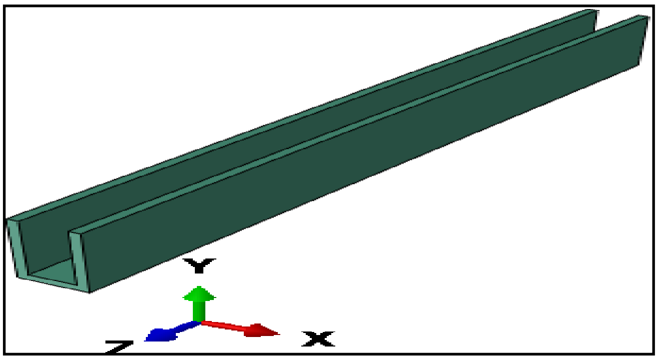

Figure 5. SIFCON layer.

2.2. Materials

2.2.1. Concrete

In a model of simple linear elasticity for isotropic concrete materials, the material constants are Young's modulus of elasticity (E_c) = 25000 MPa and Poisson's ratio (v) = 0.15. Lee and Fenves improved the concrete damaged plasticity (CDP) model [10]. The CDP model is employed in the ABAQUS manual, used in Table 1 [11].

Table 1. The parameters of the concrete damaged plasticity models.

Plasticity	Default
Dilation angle (Ψ)	30-45
Eccentricity (€)	0.1
fb0/fc0	1.16
K	0.667
Viscosity parameter (μ)	0.001

2.2.2. Steel reinforcement

In ABAQUS, the behavior of the steel reinforcement is expressed as a bilinear elastic-plastic curve. Bond slip is not considered in the embedded region modeling approach, according to [12]. Agree with ASTM A1064 and A615 G 60 [13, 14], the elastic modulus (E_c) =200000 MPa and Poisson's ratio (v) =0.15. Steel reinforcement properties given in Table 2.

Table 2. Steel reinforcement properties.

D (mm)	F_y (MPa)	F_u (MPa)	Elongation (%)
8	425.3	680.1	18.1
ASTM A1064	515	585	9
10	524	687	13
12	530	681	12
ASTM A615	420	620	9

2.2.3. Defining SIFCON material behavior

SIFCON material is a composite of concrete and fiber, it may give more compressive strength compared with NC, some properties can be directly and others indirectly. The difference factor between SIFCON and NC is not only compressive strength but also an increase in tensile strength. There is a number of studies that investigated the differences between fiber concrete and NC in FEs. It is suggested that tension stiffening represents this difference [15].The used models in literature are Scanlon-Murray model, Lin and Scordelis model, Vebo and Ghali model, and Gilbert and Warner model [16]. Fiber concrete has stress-strain properties that are pretty comparable to NC. They exhibit initially elastic behavior, which is followed by yielding and strain to harden. Additionally, the model uses these curves in a lack of stress-strain data. The stress-strain relationship for NC is modeled by an Excel sheet. The SIFCON mechanical behavior of compression and tension will be comparable. The tension stiffening model is shown in Fig. 6. In the same way as above, the SIFCON materials are defined by known tension stiffening from the Lin and Scordelis model [16]. Table 3 shows the properties of NC and SIFCON given from the test that occurred in Al-Nahrain University Laboratories.

Table 3. Normal concrete and SIFCON properties.

Mix	f′c	fcu	fr	fct	E
Normal	28.35	35.64	4.044	3.901	25000
5 % SF	57.56	70.23	7.525	6.910	37200
(4 % SF + 1 % GF)	48.13	58.69	4.616	4.500	35250
(3 % SF + 2 % GF)	44.97	54.85	3.781	3.725	34500
(2.5 % SF + 2.5 % GF)	37.40	46.32	3.451	3.423	32450
(2 % SF + 3 % GF)	33.50	40.81	3.210	2.943	31725

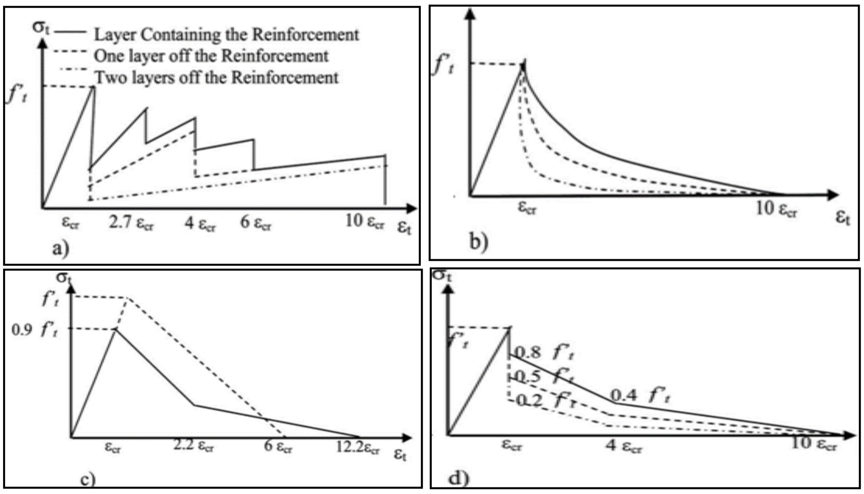

Figure 6. Various models of tension stiffening: a) Scanlon-Murray model; b) Lin and Scordelis model; c) Vebo and Ghali model; and d) Gilbert and Warner model [16].

2.3. Sections

Each material in ABAQUS needs the definition of a section. A section describes the characteristics or region of a part [17]. The section involving a concrete part, SIFCON, loader, bracket, and support is defined as a "solid homogeneous" section. A truss section was assigned for the steel reinforcement part, defined by the cross-sectional area. In addition, the second objective of the section assignment is to associate the desired material with the element [18].

2.4. Assembling of Components

Using an assembly module, each item developed in the simulation model was gathered in a coordinate system and made independent of the other elements of the model, Figs. 7 to 9.

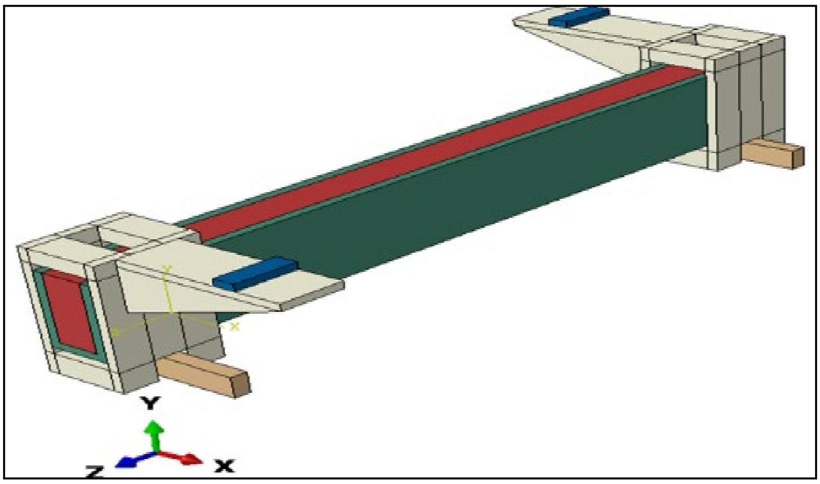

Figure 7. Assembly of the beam parts.

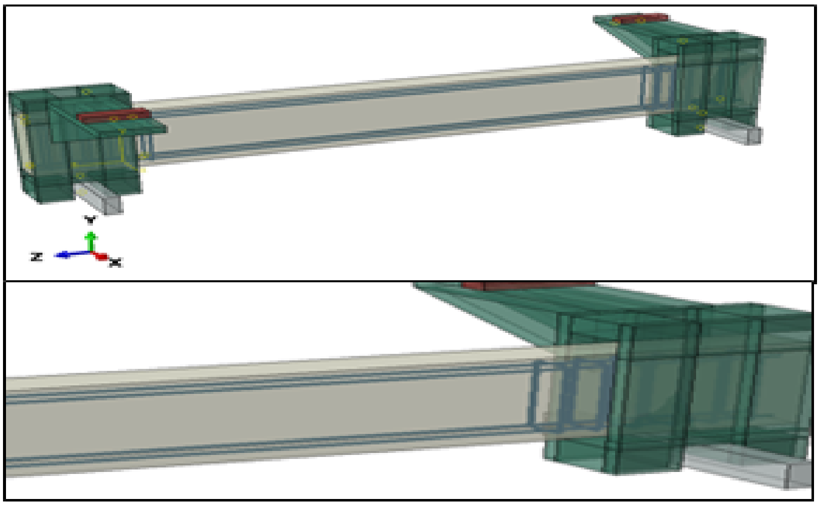

Figure 8. Assembling of the beam (BN).

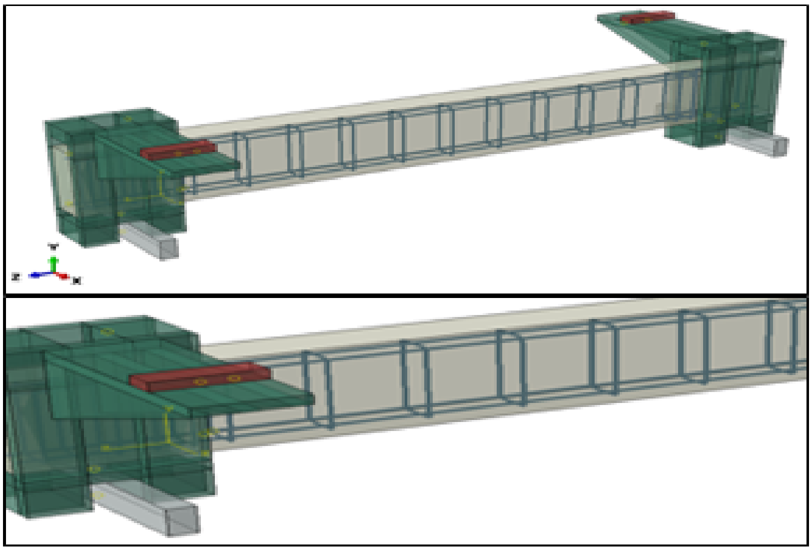

Figure 9. Assembling of the beam (BW).

2.5. Constraints and Interaction

A steel-to-concrete connection is required for RC construction. This contact permits longitudinal forces from the reinforcement to be transmitted to the surrounding concrete and vice versa. ABAQUS provides several constitutive models for representing surface interactions [19].

For bonding the loader with bracket, support with bracket, and concrete beam with bracket by using (General Contact) surface to surface contact (Standard) with step-1 and from General Contact. Based on the characteristics of the interaction kind of contact, choose two categories 1-normal behavior (Hard Contact), 2-tangential behavior with the penalty, and the coefficient of friction are equal (0.35) [18]. Furthermore, an embedded region constraint is used to represent the interaction between the steel reinforcement and the concrete section, and welded parts of the bracket by tie constrains interaction. A full bond with no relation slip between the SIFCON layer and RC beam by using (General Contact) surface-to-surface contact (Standard) with step-1 and from General Contact. In addition, for the loading arm, the alternative "rigid body" constraint type is employed. To change the arm's deformability into its non-deformability.

2.6. Meshing

Meshing is a common occurrence in every model that must be simulated using the FE approach. ABAQUS has several components and forms, each designed for a certain simulation application [20]. The numerical model's mesh size is shown in Fig. 10. A mesh sensitivity analysis to obtain the optimum mesh size considering beam behavior and element sizes 25, 35, 50 mm was performed as shown in Fig. 11.

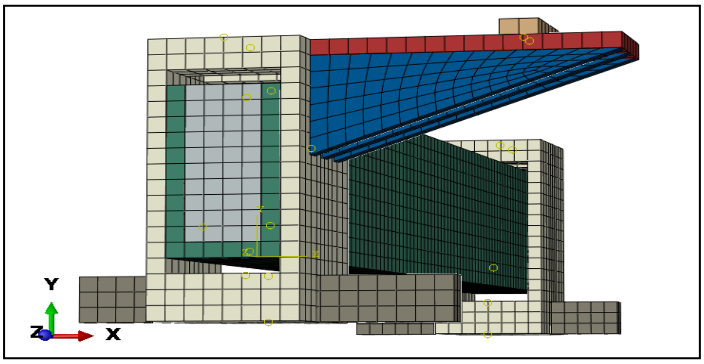

Figure 10. Mesh sensitivity study.

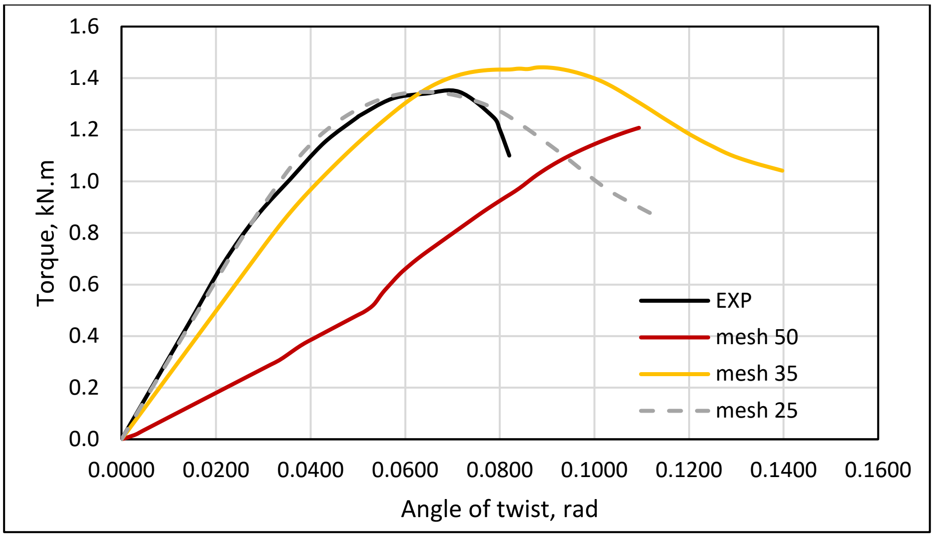

Figure 11. Meshing of the beam.

2.7. Loading and Boundary Conditions

In structural analysis, ABAQUS supports a variety of techniques and capabilities for applying mechanical, thermal, or a combination of the two. Automatic loading can generally be defined by forces, inertia forces (as gravity), pressures, and specified displacements. The load was applied in this process as a downward displacement (displacement/rotation) on the loading arm same as experimental program. The chosen approach is advised by many academics since it can solve the majority of these convergence issues. As shown in Fig. 12, to restrict beams, one types of supports are used pinned supports, which only permit rotation and restrict both vertical and longitudinal movement [21].

2.8. Type of Analysis

The static-general step analysis was used to apply loads. Only if the simulated system is not time-dependent can a static analysis be performed [22]. ABAQUS/Standard by default uses a period, in which "time" varies between 0.0 and 1.0 across the stage. To offer the program a greater range for picking the correct increment number, the maximum number of increments given was 10^4. This amount has no bearing on the analysis; it is just the maximum number of increments. The beginning and minimum increment sizes were chosen at 10^{-3} to avoid convergent issues. The maximum increment size was set to a value of 10^{-1}. The automated stabilization defined a dissipated energy percentage of 0.0002 to achieve static-general analysis.

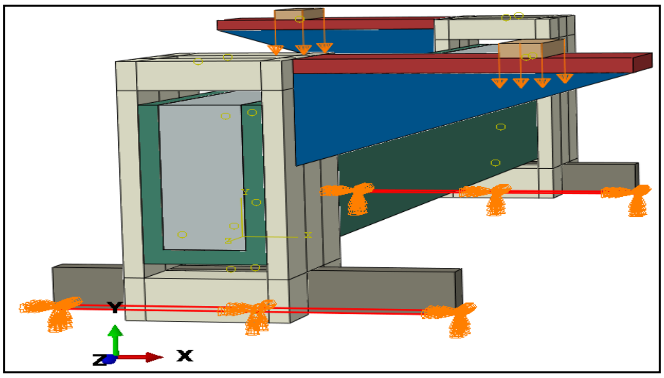

Figure 12. Beam boundary conditions and load.

3. *Results and Discussion*

3.1. Numerical Validation

The findings of the FE analysis are collated, organized, and presented for comparison with the experimental data, as shown in Table 4, and Figs. 13 and 14 comparisons between the ultimate torque and angle of twist finding from FE and the experimental test for the tested specimens. The values of the mean and coefficient of variations for [(Tu)FE/(Tu)Exp] were 0.998 and 0.247 %, respectively, for ultimate torque, while for the angle of twist [(Angle of twist) FE/(Angle of twist) Exp] were 0.945 and 3.823 %, respectively. The results indicate that when strengthening was used, the beam increased torsional capacity significantly.

Table 4. Numerical and experimental result.

Beams	Describe	FE		Exp. [9]		$T_u)_{FE}$ / $T_u)_{Exp}$	$\phi)_{FE}$ / $\phi)_{Exp}$
		T_u kN	ϕ Rad	T_u kN	ϕ Rad		
BN	Without torsional reinforcement	1.347	0.0635	1.347	0.07143	1.000	0.889
BW	With torsional reinforcement	2.410	0.0632	2.424	0.06429	0.994	0.983
BSSSFb	With strengthening SF 5%	5.957	0.1058	5.961	0.10909	0.999	0.970
BSSHFb	With strengthening HF (3 % + 2 %)	3.757	0.0799	3.756	0.08500	1.000	0.940
	Mean					0.998	0.945
	STDEV.					0.036148	0.002466
	C.V. %					0.247	3.823

$$C.V(\%) = \frac{STDEV.}{Mean} * 100. \tag{1}$$

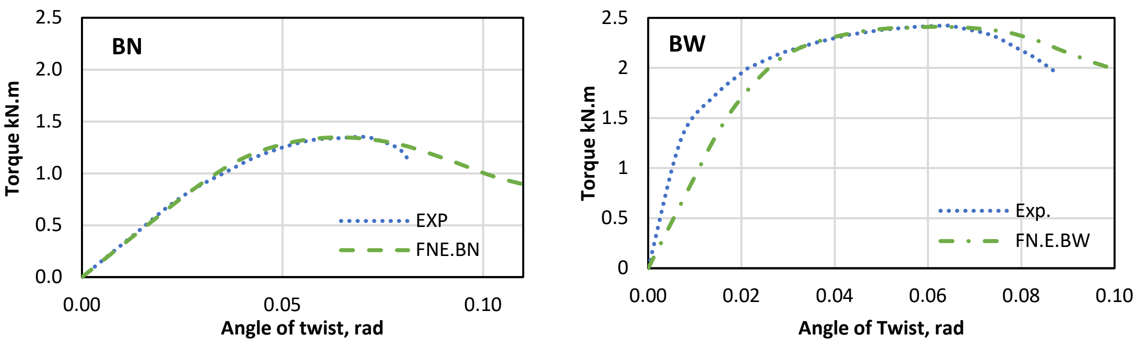

Figure 3. Numerical validation of BN and BW in ABAQUS.

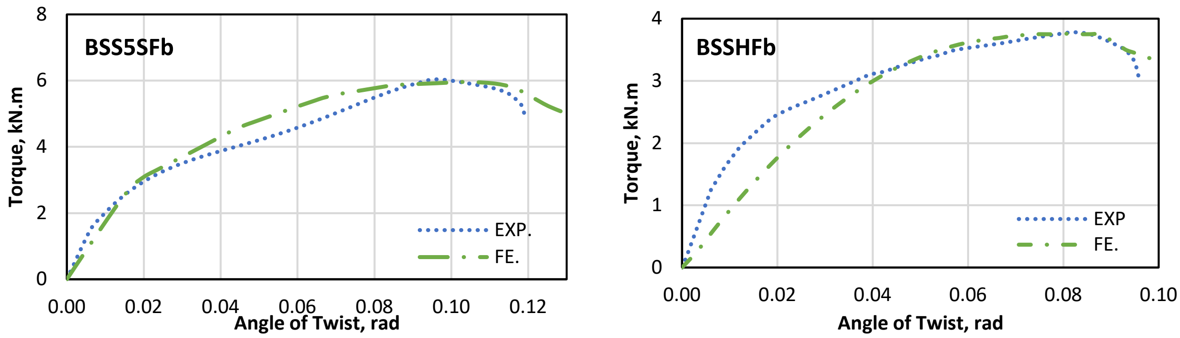

Figure 4. Numerical validation of BSS5SFb and BSSHFb in ABAQUS.

3.2. Parametric Study

3.2.1. Effect of Compressive strength of NC Beam

Three compressive strengths (CS) are chosen = 28, 38, and 48 MPa. The increase in CS led to an increase in the stiffness of beams, which led to an increase in the ultimate torque capacity. Figs. 15 to 17 show the effect of the CS of NC beams on the ultimate torque capacity and the torque and angle of twist relation. Table 5 illustrates that the increase in the ultimate torque capacity is 1 and 6 % for beams FE.BN-38 and FE.BN-48, respectively, related to beam FE.BN-28, while the percent of the increase in the ultimate torque capacity is 2 and 5 % for beams FE.BW-38 and FE.BW-48, respectively, related to FE.BW-28. The percent of the increase in the ultimate torque capacity is 0.17 and 4 % for beams FE.BSSSFb-38 and FE.BSSSFb-48, respectively, related to FE.BSSSFb-28, while the percent of the increase in the ultimate torque capacity is 1.84 and 7.13 % for beams FE.BSSHFb-38 and FE.BSSHFb-48, respectively, related to FE.BSSHFb-28. The effect was found to be marginal for the select CS range.

Table 5. Effect of compressive strength of the normal concrete beam.

Beams	Describe	T_u (kN.m)	Angle of twist	% increase in T_u
FE.BN28	Without torsional reinforcement and CS 28 MPa	1.347	0.0635	Ref1
FE.BN38	Without torsional reinforcement and CS 38 MPa	1.372	0.067	1.86
FE.BN48	Without torsional reinforcement and CS 48 MPa	1.434	0.0645	6.46
FE.BW28	With torsional reinforcement and CS 28 MPa	2.41	0.0632	Ref2
FE.BW38	With torsional reinforcement and CS 38 MPa	2.464	0.0597	2.24
FE.BW48	With torsional reinforcement and CS 48 MPa	2.55	0.0632	5.81
FE.BSSSFb28	Strengthening with 5 % SF and CS 28 MPa	5.957	0.1058	Ref3
FE.BSSSFb38	Strengthening with 5 % SF and CS 38 MPa	5.967	0.0858	0.17
FE.BSSSFb48	Strengthening with 5 % SF and CS 48 MPa	6.212	0.086	4.28
FE.BSSHFb28	Strengthening with (3 SF+2 GF)% and CS 28 MPa	3.757	0.0799	Ref4
FE.BSSHFb38	Strengthening with (3 SF+2 GF)% and CS 38 MPa	3.826	0.0742	1.84
FE.BSSHFb48	Strengthening with (3 SF+2 GF)% and CS 48 MPa	4.025	0.075	7.13

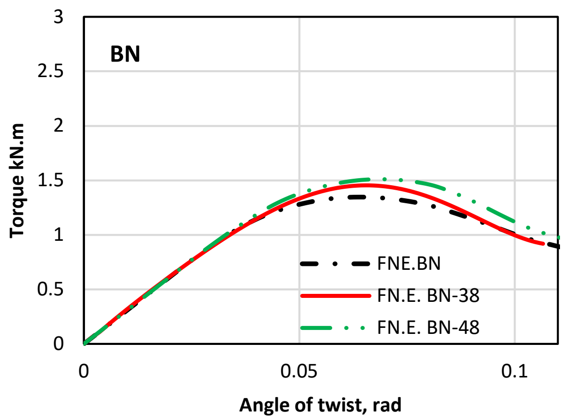

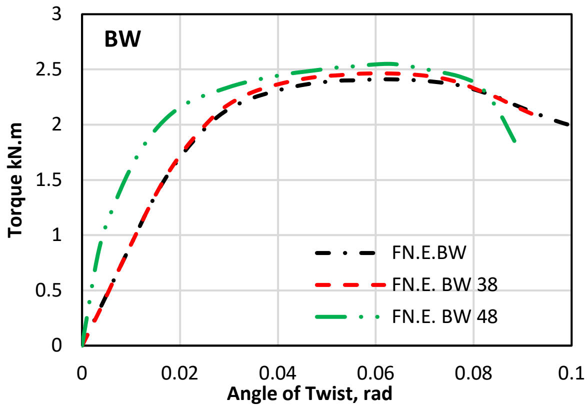

Figure 5. Torque and angle of twist relationship in ABAQUS for beams BN and BW with effect of compressive strength.

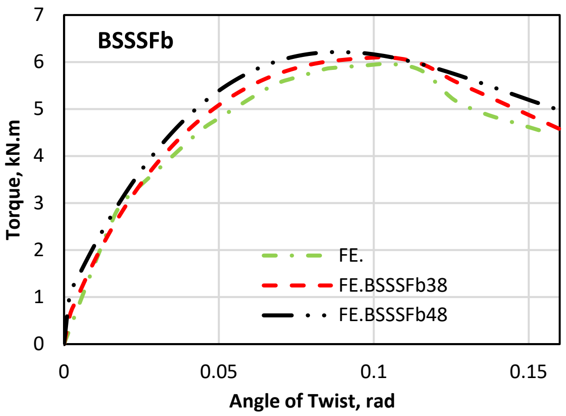

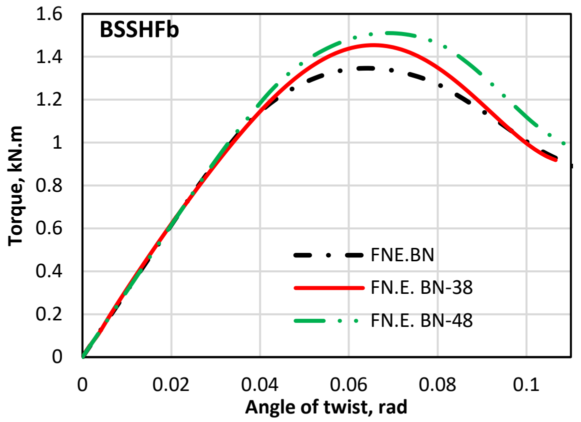

Figure 6. Torque and angle of twist relationship in ABAQUS for beams BSSSFb and BSSHFb with effect of compressive strength.

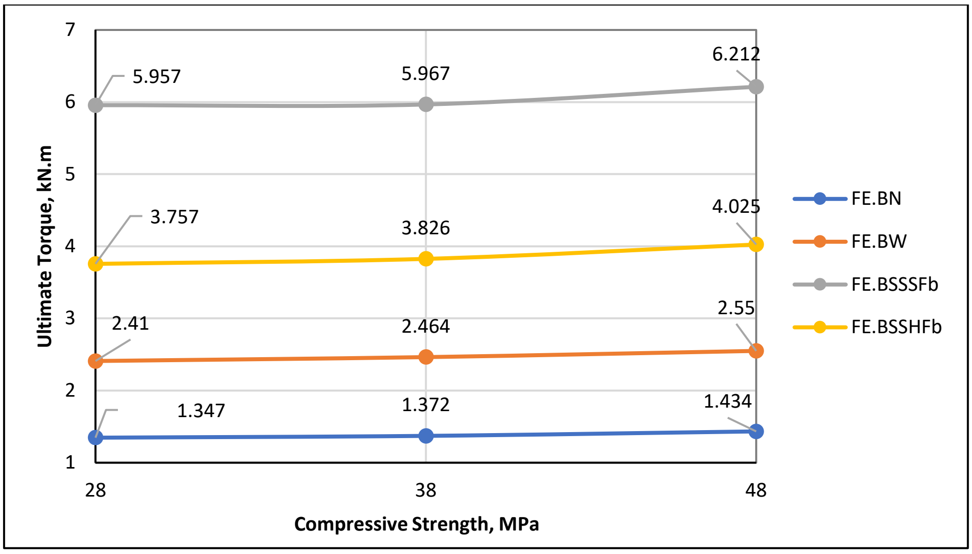

Figure 17. Effect of compressive strength on the ultimate torque capacity.

3.2.2. Effect of main reinforcement diameter – 8, 10, and 12 mm

Figs. 18 and 19 show the effect of reinforcement diameter on the ultimate torque capacity and the torque and angle of twist relative studied for beams. Three diameters were chosen = 8, 10, and 12 mm. The increase in reinforcement bar diameter led to a rise in the ultimate torque capacity. Table 6 illustrates that the increase in the ultimate torque capacity is about 8 and 12 % for beams FE.BN-10 and FE.BN-12, respectively, related to FE.BN, while the percent of the increase in the ultimate torque capacity is 4.02 and 11.66 % for beams FE.BW-10 and FE.BW-12, respectively, related to FE.BW. The percent of the increase in the ultimate torque capacity is 1.93 and 4.45 % for beams FE.BSSSFb-10 and FE.BSSSFb-12, respectively, related to FE.BSSSFb, while the percent of the increase in the ultimate torque capacity is 2.66 and 5.32 % for beams FE.BSSHFb-10 and FE.BSSHFb-12, respectively, related to FE.BSSHFb. Fig. 20 shows the effect of reinforcement diameter on the ultimate torque capacity.

Table 6. Effect of reinforcement diameter (8, 10, and 12 mm).

Beams	Describe	T_u (kN.m)	Angle of twist (rad)	% increase in T_u
FE.BN8	Without torsional reinforcement and CS 28 MPa	1.347	0.0635	Ref1
FE.BN10	Without torsional reinforcement and CS 38 MPa	1.454	0.0653	7.94
FE.BN12	Without torsional reinforcement and CS 48 MPa	1.51	0.069	12.10
FE.BW8	With torsional reinforcement and CS 28 MPa	2.41	0.0632	Ref2
FE.BW10	With torsional reinforcement and CS 38 MPa	2.507	0.0632	4.02
FE.BW12	With torsional reinforcement and CS 48 MPa	2.691	0.0606	11.66
FE.BSSSFb8	Strengthening with 5 % SF and CS 28 MPa	5.957	0.1058	Ref3
FE.BSSSFb10	Strengthening with 5 % SF and CS 38 MPa	6.072	0.09983	1.93
FE.BSSSFb12	Strengthening with 5 % SF and CS 48 MPa	6.222	0.09982	4.45
BSSHFb8	Strengthening with (3 SF+2 GF) % and CS 28 MPa	3.757	0.0799	Ref4
FE.BSSHFb10	Strengthening with (3 SF+2 GF) % and CS 38 MPa	3.857	0.0818	2.66
FE.BSSHFb12	Strengthening with (3 SF+2 GF) % and CS 48 MPa	3.957	0.0799	5.32

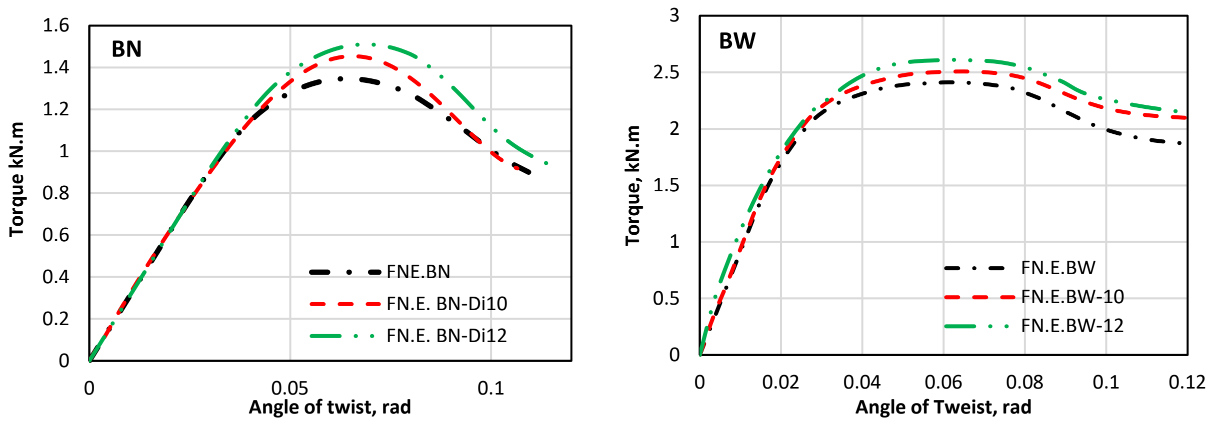

Figure 7. Torque and angle of twist relationship ABAQUS for beams BN and BW.

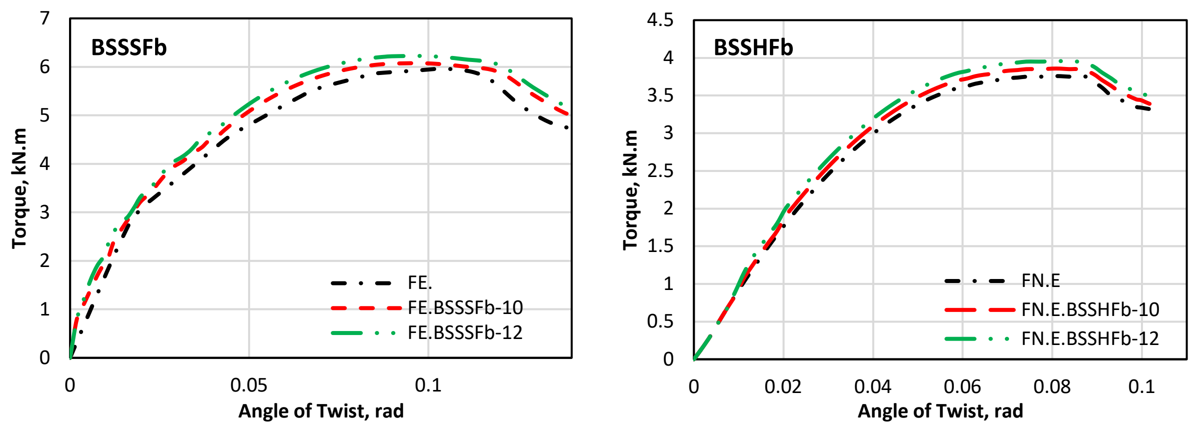

Figure 8. Torque and angle of twist relationship ABAQUS for beams BSSSFb and BSSHFb with variable reinforcement.

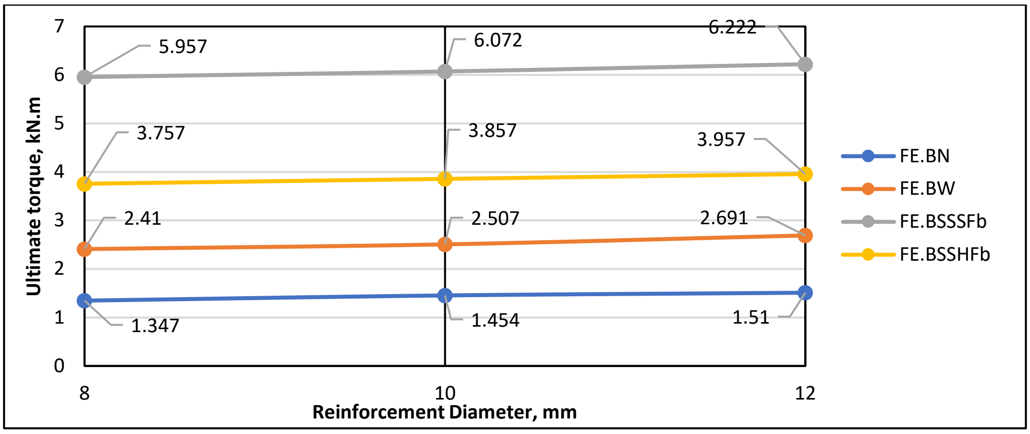

Figure 20. Effect reinforcement diameter on ultimate torque capacity.

3.2.3. Effect of thickness of the SIFCON layer (25, 15, and 35 mm)

Figs. 21 and 22 show the effect of thickness of the SIFCON layer on the ultimate torque capacity and the torque and angle of twist relation was studied for beams. Three thicknesses of the SIFCON layer values – 15, 25, and 35 mm. The increase in the thickness of the SIFCON layer leads to an increase in the ultimate torque capacity, while decreasing in the thickness of the SIFCON layer leads to a decrease in the ultimate torque capacity. Table 7 illustrates the increase and decrease in the ultimate torque capacity. When using the thickness of 35 mm percent the increase in the ultimate torque capacity is about 6, and 7 % for beams FE.BSSSFb-t35 and FE.BSSHFb-t35, respectively, while using the thickness of layet 15 mm, the ultimate torque decrease about 17, and 3 % related to beams FE.BSSSFb-t15 and FE.BSSHFb-t15, respectively. Figs.21 and 22 show the effect of thickness of the SIFCON layer on the ultimate torque capacity.

Table 7. Effect of thickness of the SIFCON layer (25, 15, and 35 mm).

Beams	Describe	T_u (kN.m)	Angle of twist (rad)	% increase in T_u
FE.BSSSFb-t25	Beam strengthening with 5 % SF and thickness 25 mm	5.957	0.1058	Ref1
FE.BSSSFb-t15	Beam strengthening with 5 % SF and thickness 15 mm	4.934	0.08583	–17.17
FE.BSSSFb-t35	Beam strengthening with 5 % SF and thickness 35 mm	6.288	0.0958	5.56
FE. BSSHFb-t25	Beam strengthening with (3SF+2GF) % and thickness 25 mm	3.757	0.0799	Ref2
FE.BSSHFb-t15	Beam strengthening with (3SF+2GF) % and thickness 15 mm	3.651	0.0732	–2.82
FE.BSSHFb-t35	Beam strengthening with (3SF+2GF) % and thickness 35 mm	4.001	0.0747	6.49

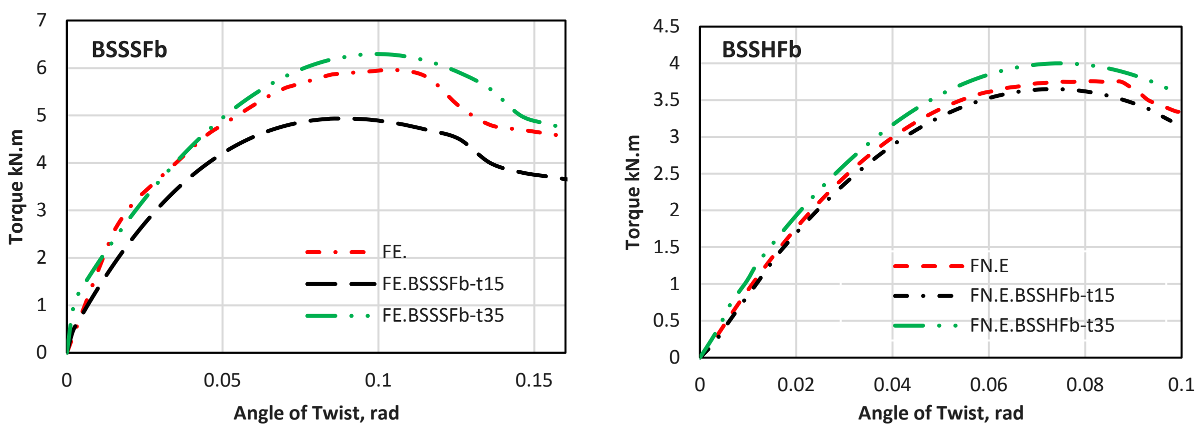

Figure 21 Torque and angle of twist relationship ABAQUS for beams BSSSFb and BSSHFb with variable SIFCON thickness.

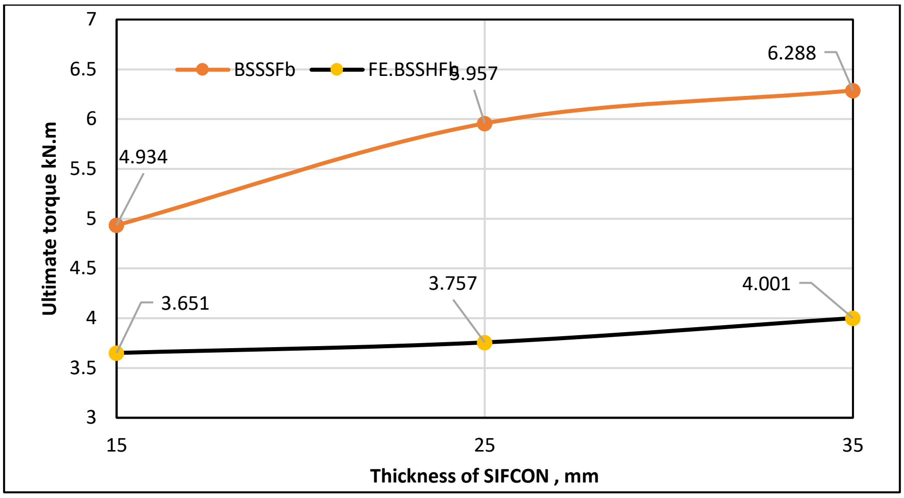

Figure 22. Effect of thickness of the SIFCON layer on the ultimate torque capacity.

3.2.4. Effect of hybrid fiber (SF + GF) (3 % + 2 %, 2.5 % + 2.5 %, and 2 % + 3%)

Fig. 23 shows the effect of HF of the SIFCON layer on the ultimate torque capacity and the torque and angle of twist relation studied for beams. Three HF of the SIFCON layer values (SF+GF) (3 % + 2 %, 2.5 % + 2.5 %, and 2 % + 3%). The decrease in SF in HF led to a decrease in the ultimate torque capacity. Table 8 shows that the decrease in the ultimate torque capacity is about 9 and 17 % for beams FE.BSSHFc and FE.BSSHFd, respectively.

Table 8. Effect of hybrid fiber.

Beams	Describe	Tu (kN.m)	Angle of twist (rad)	% increase of Tu
FE.BSSHFb	HF (3% SF + 2% GF)	5.957	0.0799	Ref1
FE.BSSHFc	HF (2.5% SF + 2.5% GF)	5.436	0.0958	8.75
FE.BSSHFd	HF (2% SF + 3% GF)	4.934	0.0858	17.17

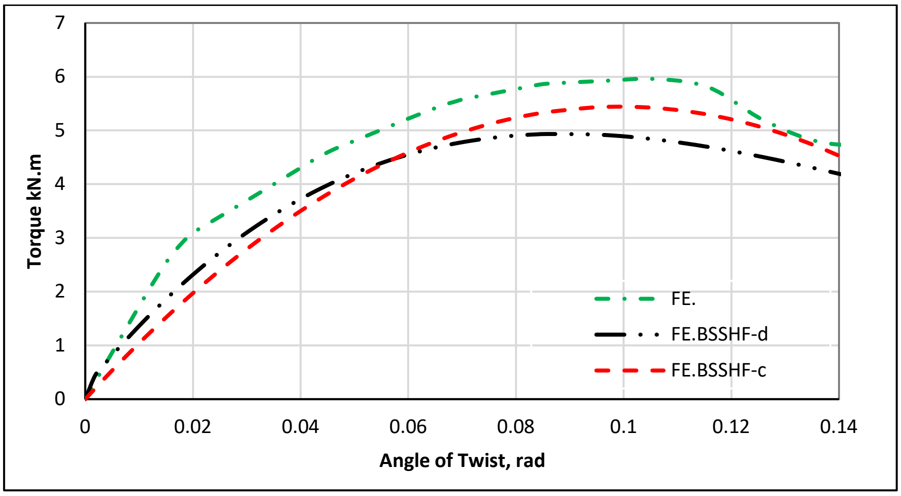

Figure 93. Torque and angle of twist relationship ABAQUS for beams BSSHFb with variable ratios of hybrid fiber.

3.2.5. Effect of length of the SIFCON layer (2 and 1.5 m)

Fig. 24 shows the effect of length of the SIFCON layer on the ultimate torque capacity and the torque and angle of twist relation was studied for beams. Two length of the SIFCON layer values = 2 and 1.5 m. The decrease in the length of the strengthening layer led to a decrease in the ultimate torque capacity. Table 9 shows that the decrease in the ultimate torque capacity is about 21 and 12 % for beams FE.BSSHFc and FE.BSSHFd, respectively.

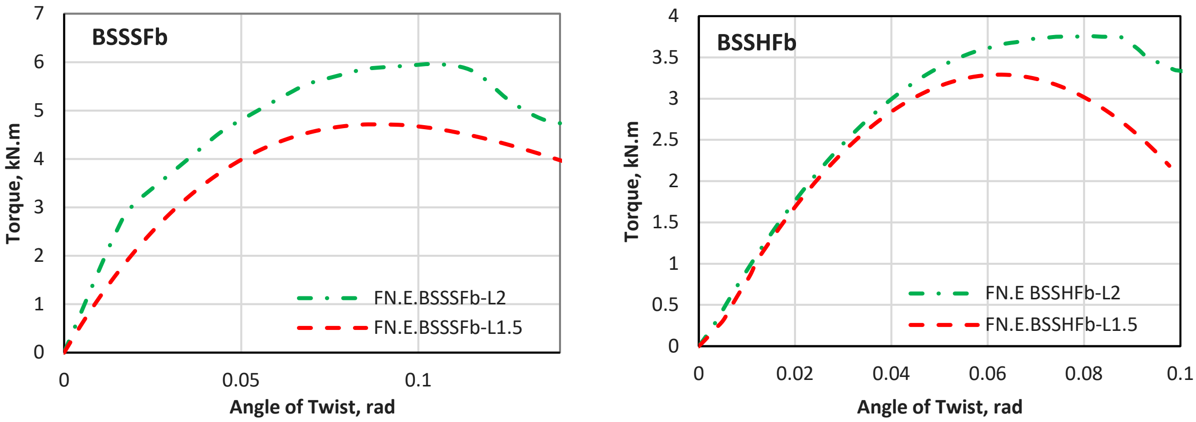

Figure 24. Torque and angle of twist relationship from ABAQUS for beams BSSSFb and BSSHFb.

Table 9. Effect of length of the SIFCON layer (2 and 1.5 m).

Beams	Describe	Tu (kN.m)	Angle of twist (rad)	% increase of Tu
F.E.BSSSFb-L2	Length of strengthening layer 2 m	5.957	0.1058	Ref1
FN.E.BSSSFb-L1.5	Length of strengthening layer 2 m	4.714	0.0858	–20.87
F.E.BSSHFb-L2	Length of strengthening layer 2 m	3.757	0.0799	Ref2
FN.E.BSSHFb-L1.5	Length of strengthening layer 2 m	3.29	0.0619	–12.43

3.3. Failure Mode

The failure mode in the torque is always cracks inclined at 45 degrees, appearing on both sides [23]. The cracks in the ABAQUS program are often more numerous and larger than they are experimentally because the program also shows invisible cracks as clear, as can be seen in Fig. 25.

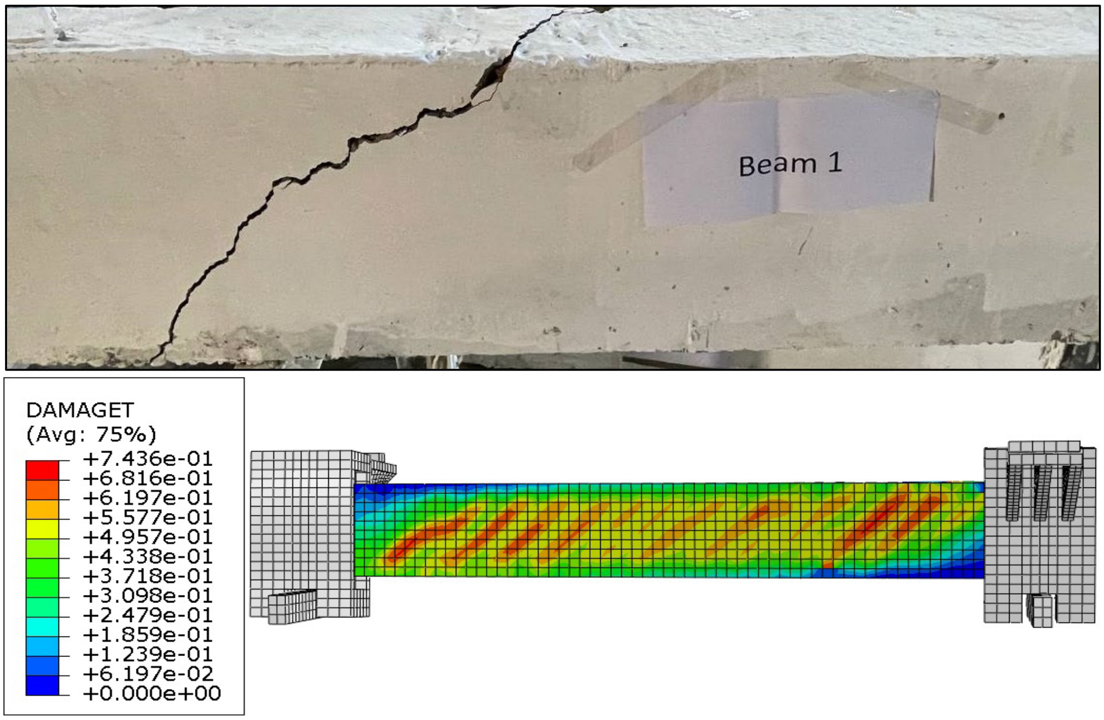

Beam BN

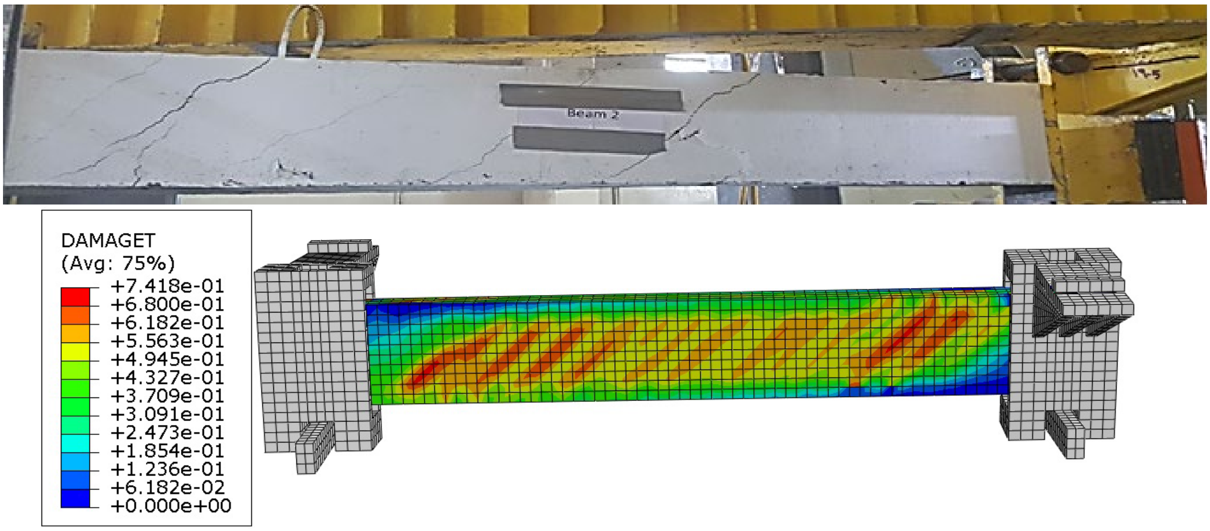

Beam BW

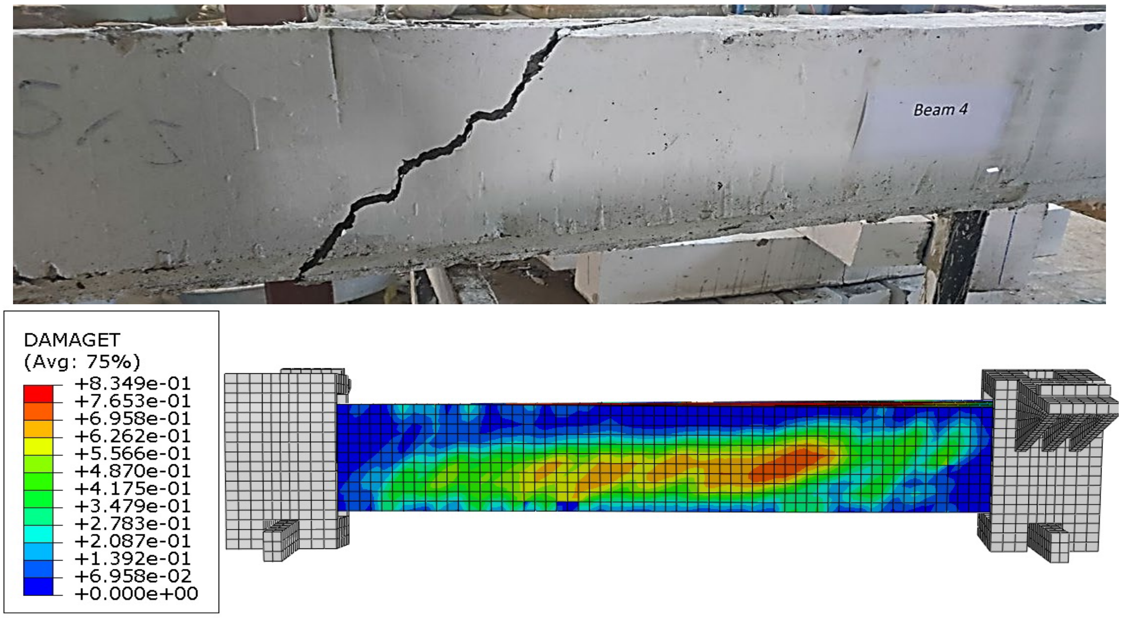

Beam BSSSFb

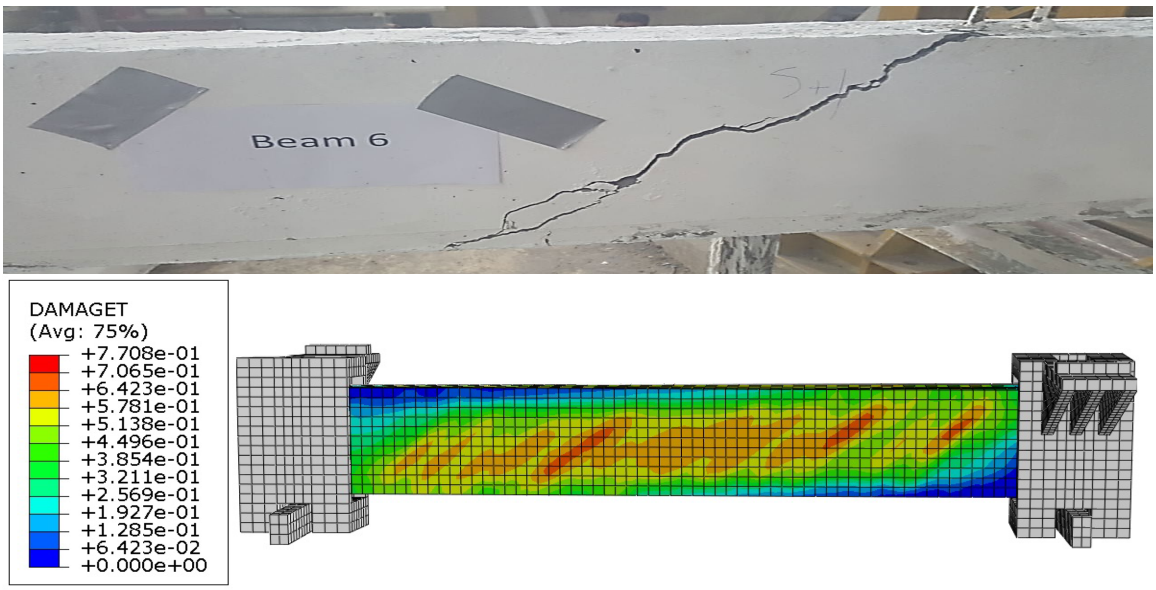

Beam BSSHFb

Figure 25. Damage tensile under pure torsion for tested beams.

4. Conclusions

The following conclusions are obtained from FE analysis:

1. Reasonable agreement was acquired between the ultimate torque and angle of twist of FE numerical models and found experimentally, in which the value of the mean and coefficient of variations were 0.998 and 0.247 %, respectively, for the ultimate torque, whilst, for the angle of twist, the value of the mean and coefficient of variation were 0.945 and 3.823 %, respectively.
2. The effect of CS on the ultimate torque capacity was studied numerically, the percentage of the increase in the ultimate torque capacity is 1 and 6 % for the reference beams without torsional reinforcement having the CSs of 38 and 48 MPa, respectively. The percent of the increase in the ultimate torque capacity is 2 and 5 % for the reference beams with torsional reinforcement having CSs of 38 and 48 MPa, respectively. The percent of the increase in the ultimate torque capacity is 0.17 and 4 % for three-sided SF SIFCON beams having CSs of 38 and 48 MPa, respectively. The percent of the increase in the ultimate torque capacity is 1.84 and 7.13 % for three-sided HF SIFCON beams having CSs of 38 and 48 MPa, respectively. The increase is marginal due to the selected range of CS.
3. The effect of increasing longitudinal reinforcement ratio is found to be higher for the torsionally unreinforced beam and marginal for the other beams for the selected range of reinforcement ratio or diameter (8 to 12 mm bar diameter).
4. The effect of thickness of the SIFCON layer on the behavior is found to be higher for SF SIFCON and lower for HF SIFCON jacketing.
5. The effect of HF on behavior is studied. It is clear that the decrease in SF content in HF SIFCON led to a decrease in the ultimate torque capacity. The decrease in the ultimate torque capacity is about 9 and 17 % for SIFCON beams with (2.5 SF + 2.5 GB) % and (2 SF + 3 GB) %, respectively.
6. It is clear that the decrease in the length of the SIFCON strengthening layer led to a decrease in the ultimate torque capacity. The decrease in the ultimate torque capacity is about 21 % for beams with strengthened SF SIFCON and 12 % for beams with HF SIFCON jacketing.
7. The increase depends on the type of parameter, whether it is primarily within the strengthening or secondary (parameter that effects on torsion not strengthening), as increasing the CS of the core beam is considered a secondary parameter, and the increase may be small. As for the primary parameters that affect the study of strengthening, for example, changing the thickness, percentage of fibers, and length of the reinforcement layer, they have a clear fundamental effect.

References

1. Andersen, P. Experiments with concrete in torsion. Transactions of the American Society of Civil Engineers. 1935. 100(1). Pp. 949–960.
2. Bentur, A., Cree, R. Cement reinforced with steel wool. International Journal of Cement Composites and Lightweight Concrete. 1987. 9(4). Pp. 217–223.
3. Ipek, M., Aksu, M. The effect of different types of fiber on flexure strength and fracture toughness in SIFCON. Constr. Build. Mater. 2019. 214. 207–218. DOI: 10.1016/j.conbuildmat.2019.04.055
4. Ali, M.I., Al-Azzawi, A.A. Finite element analysis of RC beams strengthened with near-surface mounted reinforcement bars under pure torsion. IOP Conference Series: Earth and Environmental Science. 2023. 1232(1). 12026. DOI: 10.1088/1755-1315/1232/1/012026
5. Le, K.B., Van Cao, V. Numerical Study of Circular Concrete Filled Steel Tubes Subjected to Pure Torsion. Buildings. 2021. 11(9). Article no. 397. DOI: 10.3390/buildings11090397
6. Majed, M.M., Tavakkolizadeh, M., Allawi, A.A. Finite element analysis of rectangular RC beams strengthened with FRP laminates under pure torsion. Structural Concrete. 2021. 22(4). Pp. 1946–1961. DOI: 10.1002/suco.202000291
7. Ganganagoudar, A., Mondal, T.G., Prakash Shanmugam, S. Analytical and finite element studies on behavior of FRP strengthened RC beams under torsion. Composite Structures. 2016. 153. Pp. 876–885. DOI: 10.1016/j.compstruct.2016.07.014
8. Jain, S., Chellapandian, M., Prakash Shanmugam, S. Emergency repair of severely damaged reinforced concrete column elements under axial compression: An experimental study. Construction and Building Materials. 2017. 155. 751–761. DOI: 10.1016/j.conbuildmat.2017.08.127
9. Mohammed, J.M. Torsional Performance of Reinforced Concrete Beams Strengthened with SIFCON Jacketing., MSc. Thesis, Department of Civil Engineering, College of Engineering, Al-Nahrain University, 2024.
10. Le Thanh, C., Minh, H.L., Sang-To, T. A nonlinear concrete damaged plasticity model for simulation reinforced concrete structures using ABAQUS. Frattura ed Integrità Strutturale. 2022. 16(59). Pp. 232–242. DOI: 10.3221/IGF-ESIS.59.17
11. ABAQUS. ABAQUS Analysis User's Manual Version 6.13. Rensselaer Polytechnic Institute, 2013.
12. Malm, R. Shear Cracks in Concrete Structures Subjected to In-Plane Stresses. Licentiate Thesis. KTH Royal Institute of Technology, 2006. 136 p.
13. ASTM A1064/A1064M-14. Standard Specification for Carbon-Steel Wire and Welded Wire Reinforcement, Plain and Deformed, for Concrete. ASTM International. West Conshohocken, PA, 2020.

14. ASTM A615/A615M-20. Standard Specification for Deformed and Plain Carbon-Steel Bars for Concrete Reinforcement. West Conshohocken, PA, 2020.
15. Padmarajaiah, S.K., Ramaswamy, A. A finite element assessment of flexural strength of prestressed concrete beams with fiber reinforcement. Cement and Concrete Composites. 2002. 24(2). Pp. 229–241. DOI: 10.1016/S0958-9465(01)00040-3
16. Wahalathantri, B., Thambiratnam, D., Chan, T., Fawzia, S. A material model for flexural crack simulation in reinforced concrete elements using ABAQUS. Proceedings of the First International Conference on Engineering, Designing and Developing the Built Environment for Sustainable Wellbeing. Queensland University of Technology. Brisbane, Qld, 2011. Pp. 260–264.
17. Khennane, A. Introduction to Finite Element Analysis Using MATLAB® and Abaqus. CRC Press, 2013. 453 p. DOI: 10.1201/b15042
18. Ali, M.I. Torsional Performance of Reinforced Concrete Beams Strengthened with Near-Surface Mounted Steel Bars. Al-Nahrain University, 2023.
19. Börgesson, L. Abaqus. Developments in Geotechnical Engineering. 1996. 79. Pp. 565–570. Pp. 10.1016/S0165-1250(96)80047-2
20. Barbero, E.J. Finite Element Analysis of Composite Materials using Abaqus®. CRC Press, 2023. 571 p. DOI: 10.1201/9781003108153
21. El-Mandouh, M.A., Hu, J.W., Shim, W.S., Abdelazeem, F., ELsamak, G. Torsional improvement of RC beams using various strengthening systems. Buildings 2022. 12(11). Article no. 1776. DOI: 10.3390/buildings12111776
22. Sun, Y. A Structural Optimization Scripted Software System. Virginia Tech, 2019. https://www.semanticscholar.org/paper/A-Structural-Optimization-Scripted-Software-System-Sun/e664ba6ccfe9fd30d3b4cfe142fd779958eb44ae
23. Hou, N., Ding, N., Qu, Sh., Guo, W., et al. Failure modes, mechanisms and causes of shafts in mechanical equipment. Engineering Failure Analysis. 2022. 136. Article no. 106216. DOI: 10.1016/j.engfailanal.2022.106216

Information about the authors:

Mohammed Mohammed*,*
E-mail: st.mohammed.g.m.f@nahrainuniv.edu.iq

Adel Al-Azzawi*,*
E-mail: dr_adel_azzawi@yahoo.com

Received 08.06.2024. Approved after reviewing 23.12.2025. Accepted 15.01.2026.